An integrated in vitro and in situ study of kinetics ofmyosin II from frog skeletal muscle

SUPPLEMENTARY MATERIAL

1. Protocol to prevent actin contamination and proteolytic degradation of frog myosin

In the incubation solution for muscle dissection (KPi (KH_2PO_4 and K_2HPO_4) 170 mM, EGTA 5 mM, Na_2ATP 2.5 mM, $MgCl_2$ 5 mM, Imidazole 10 mM, pH 7) EGTA was present to prevent uncontrolled activation initiated by Ca^{2+} release on rupture of the sarcoplasmic reticulum membrane and to reduce the level of actin contamination in the final preparation below a measurable level (compare lanes 3 and 4 in Figure S1A). The proteolytic activity in the frog skeletal muscle is a major limitation in getting intact myosin molecules. As a result, the light chains LC1 (25 kDa) and LC2 (20 kDa) get cleaved into smaller peptides LC1' (23 kDa) and LC2' (18 kDa) (Focant and Huriaux, 1980; Pliszka et al., 1978). We confirmed this degradation process in our initial extraction trials. During the purification protocol, myosin molecules with cleaved light chains polymerised with intact myosin molecules, thus preventing separation of the two. Also proteases precipitated with myosin and a slow proteolytic activity was observed during storage. The best way to prevent cleavage of subunits was by adding an antiprotease cocktail (1 tablet/50 ml, Roche Complete®) to all the solutions throughout the extraction protocol and storage. The preservation of myosin heavy chain from proteolytic degradation was tested by running 8% SDS gel electrophoresis (18 cm, long slab) for 12 hours at constant voltage of 100 mV. As shown in Figure S1B, the myosin heavy chain run as a single separate band, without any additional contaminating band due to cleaved heavy chains.

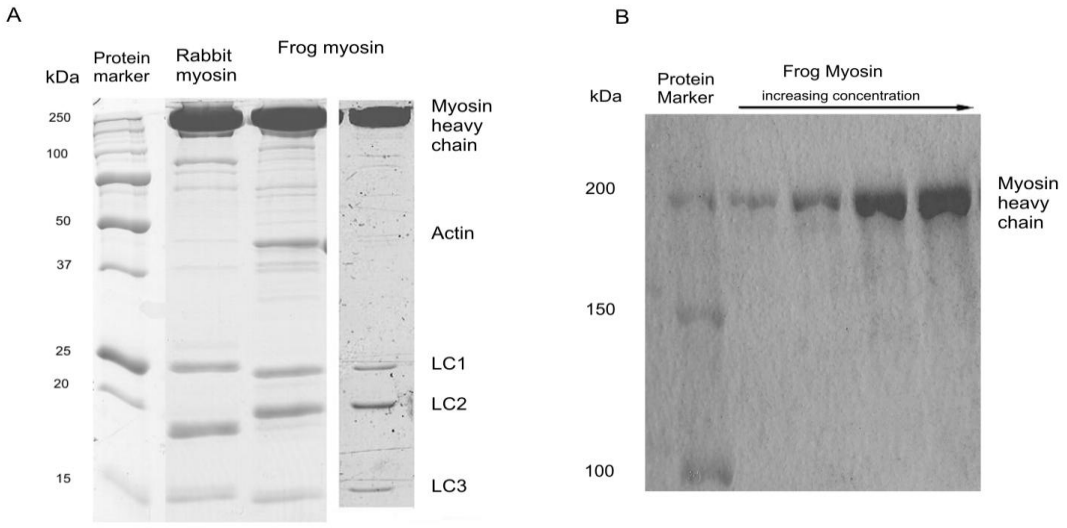

Figure S1. Polyacrylamide-gel electrophoresis (PAGE) of frog myosin in the presence of 0.1%. sodium dodecyl sulphate (SDS). **A**. 15% w/v SDS-PAGE. Lane 1: protein marker; lane 2: rabbit

myosin for comparison; lane 3: frog myosin obtained in earlier trials, without EGTA in the incubating solution; lane 4: frog myosin obtained with incubating solution with EGTA. Note in this case the absence of actin. **B**: 8% SDS page. Lane1: Protein marker; lanes 2-5: frog myosin heavy chain band obtained with increasing concentrations (range 0.5-5 μg).

2. Solutions in various experimental conditions

Base Buffer Condition	Ionic strength (mM)	Temperature (°C)	pH	KCl (mM)	Imidazole (mM)	$MgCl_2$ (mM)	EGTA (mM)	Na_2ATP (mM)	Free Mg^{2+} (mM)	CrP (mM)
Control	60 mM	23°C	7.5	35.45	25	3.07	1	2.14	1	0
pH changes										
pH 7.5	60 mM	23°C	7.5	35.45	25	3.07	1	2.14	1	0
pH 7.0	60 mM	23°C	7	28.52	25	3.02	1	2.16	1	0
pH 6.7	60 mM	23°C	6.7	22.20	25	3.01	1	2.22	1	0
Temperature changes										
5 °C	60 mM	5 °C	7.5	30.06	25	3.07	1	2.14	1	0
15 °C	60 mM	15 °C	7.5	33.02	25	3.07	1	2.14	1	0
20 °C	60 mM	20 °C	7.5	34.41	25	3.07	1	2.14	1	0
25 °C	60 mM	25 °C	7.5	35.70	25	3.07	1	2.14	1	0
30 °C	60 mM	30 °C	7.5	36.86	25	3.07	1	2.14	1	0
MgATP changes at 23 degree										
2 mM	60 mM	23 °C	7.5	34.94	25	3.07	1	2.14	1	0
1 mM	60 mM	23 °C	7.5	40.50	25	2.07	1	1.07	1	0
0.5 mM	60 mM	23 °C	7.5	4.28	25	1.57	1	0.54	1	10
0.1 mM	60 mM	23 °C	7.5	15.72	25	1.37	1	0.11	1	10
MgATP changes at 5 degree										
2 mM	60 mM	5 °C	7.5	30.06	25	3.07	1	2.14	1	0
1 mM	60 mM	5 °C	7.5	5.82	25	2.27	1	1.07	1	10
0.5 mM	60 mM	5 °C	7.5	8.59	25	1.77	1	0.54	1	10
0.1 mM	60 mM	5 °C	7.5	10.81	25	1.37	1	0.11	1	10

Table S1. List of final solutions used for IVMA measurements under different experimental conditions. The concentrations of KCl, $MgCl_2$ and Na_2ATP were adjusted to reach the final desired conditions of [MgATP] with ionic strength 60 mM.

3. IVMA data analysis.

Data analysis. Actin filament tracking was accomplished by analysing sequences of images in 16 bit format files with a custom built program in LabVIEW. Background fluorescence was excluded by setting a threshold on the intensity: the intensity was assumed to be zero in the pixels with intensity values below the threshold, whereas pixels with intensity values above threshold were unaltered. The threshold value was set so that the objects remaining in view were only actin

filaments and the noise from the background was not larger than few pixels. Filament velocity was calculated from the displacement of the actin filament centroid in two successive frames, according to the equation:

$$C_x = \frac{\sum_{i=1}^{n}\sum_{j=1}^{m}\left(x_i I_{ij}\right)}{\sum_{i=1}^{n}\sum_{j=1}^{m} I_{ij}} \quad \text{and} \quad C_y = \frac{\sum_{i=1}^{n}\sum_{j=1}^{m}\left(y_i I_{ij}\right)}{\sum_{i=1}^{n}\sum_{j=1}^{m} I_{ij}} \qquad \text{(S1)}$$

Where C_x and C_y are the centroid coordinates, x_i and y_j are the coordinates of the pixel i,j and I_{ij} is the pixel intensity.

Playing the movie backward and forward, smoothly sliding filaments were selected manually by eye and each selected filament was analysed individually. The filament was selected by choosing a rectangle around the actin filament and the number of frames to track. The position of the centroid of the filament in the first frame was calculated according to equation (S1). The position of the centroid of the same filament in the next frame was found by enlarging the filament box from the previous position and using the equation (S1) again. This tracking process was continued for all the frames selected. After determining the centroid position in successive frames, the frame-to-frame velocity of the actin movement was calculated by the distance moved between two consecutive frames multiplied by the acquisition rate (Homsher et al., 1992). The centroid position in each frame and the length of the filament (calculated by the diagonal of the rectangle bounding the filament) were stored for further analysis.

Statistical analysis of V_F. In a preliminary phase of the analysis, performed on 35 filaments, the mean sliding velocity for a given slide was calculated with two methods (see Fig. S2). The first method consisted in fitting the distribution of frame-to-frame velocities collected from all the actin filaments with a Gaussian function:

$$n = Y_0 + Ae^{\frac{(V-V_{mean})^2}{2\sigma^2}}, \qquad \text{(S2)}$$

where n is the number of measurements, V is V_F determined frame to frame, V_{mean} is the mean of the distribution, σ is the standard deviation of the distribution, and Y_0 and A are constants. The result of the fit to 458 data pooled from 35 filaments is shown in Figure S2A. The mean velocity was 5.74 ± 0.09 μm/s (mean ± SE). The second method consisted in calculating first the mean value of the

frame-to-frame velocity for each filament and then fitting the distribution of the mean filament velocities (Figure S2B). V_F in this case was 5.79 ± 0.19 μm/s. Thus, the mean values and standard deviations estimated with the two methods are the same within the experimental error. The second method was adopted for data analysis through the paper. The rationale behind this choice is that in this way we could discriminate the weight of individual filaments to the generation of V_F and, moreover, we could relate V_F of the individual filament to some other parameter of the filament, such as the filament length.

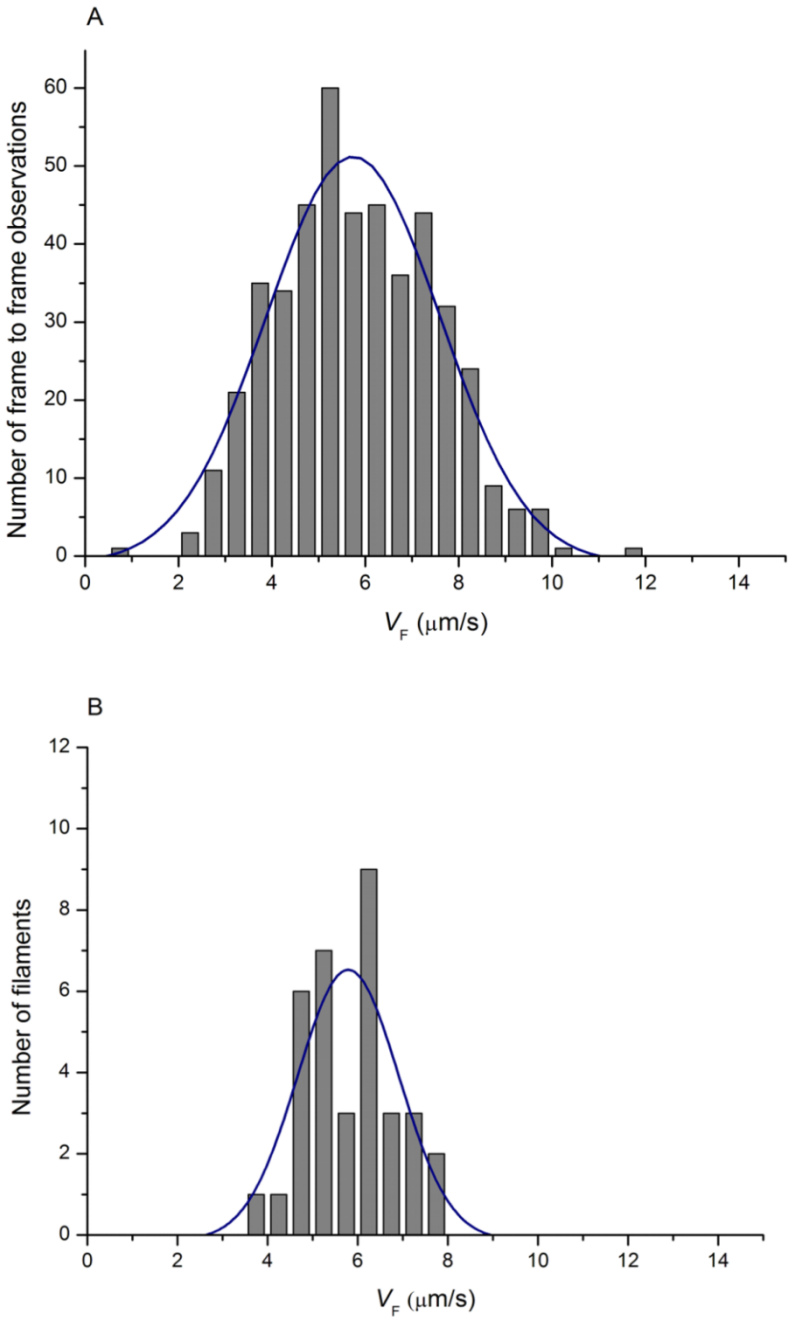

Figure S2. Histograms of observed sliding velocities (V_F, μm/s) of actin filaments over frog myosin under

control conditions. V_F is grouped in classes of 0.5 μm/s. The solid lines are the least-square fits, using a Gaussian function (4), of the number of the observations (n) as function of V_F. **A**. V_F calculated from the frame-to-frame velocity (N =458) from 35 filaments. Estimated Gaussian parameters are: mean = 5.74 μm/s and σ = 1.86 μm/s. **B.** V_F calculated as the mean velocity of each individual filament. Estimated Gaussian parameters are: mean = 5.79 μm/s and σ = 1.13 μm/s.

Sources of error. The measurement of the movement of the fluorescently labelled actin filament is affected by two kinds of error. The first kind is due to noise affecting actin localization accuracy and thus velocity evaluation. Sources of noise in the system are background fluorescence; fluctuations in the fluorescence of actin filaments due to Poisson noise and photobleaching of fluorophores attached to actin; mechanical vibrations and thermal drifts of the apparatus; electronic noise in the image acquisition system. The second kind of noise is related to uneven density and random orientation of myosin molecules and appears as occasional hesitations in filament movement, filaments halting and resuming their movement, filament buckling when the trailing end moves faster than the leading end, filament following a curved path with a narrow angle.

The system noise leads to a poor estimate of the centroid and can bias the estimate of V_F. The system noise depends on the acquisition rate: increasing the acquisition rate leads to collection of less photons per frame, thus decreasing signal-to-noise ratio (S/R) and accuracy in the estimate of the actin position. In this work the images were collected with total exposure times of 500 ms, 200 ms and 50 ms and thus at sampling rates of 2, 5 and 20 Hz respectively. As shown in Figure S3, the S/N decreased as the frame rate increased. Also the error in the estimate of the centroid position increased with increase in the frame rate. The system noise on V_F was evaluated from the SD of the centroid position of an actin filament that was immobilised by attachment to rigor myosins. From the 10 filaments analysed, we estimated the error on V_F to be 0.38 μm/s, 0.14 μm/s and 0.055 μm/s for the 20 Hz, 5 Hz and 2 Hz frame rates, respectively.

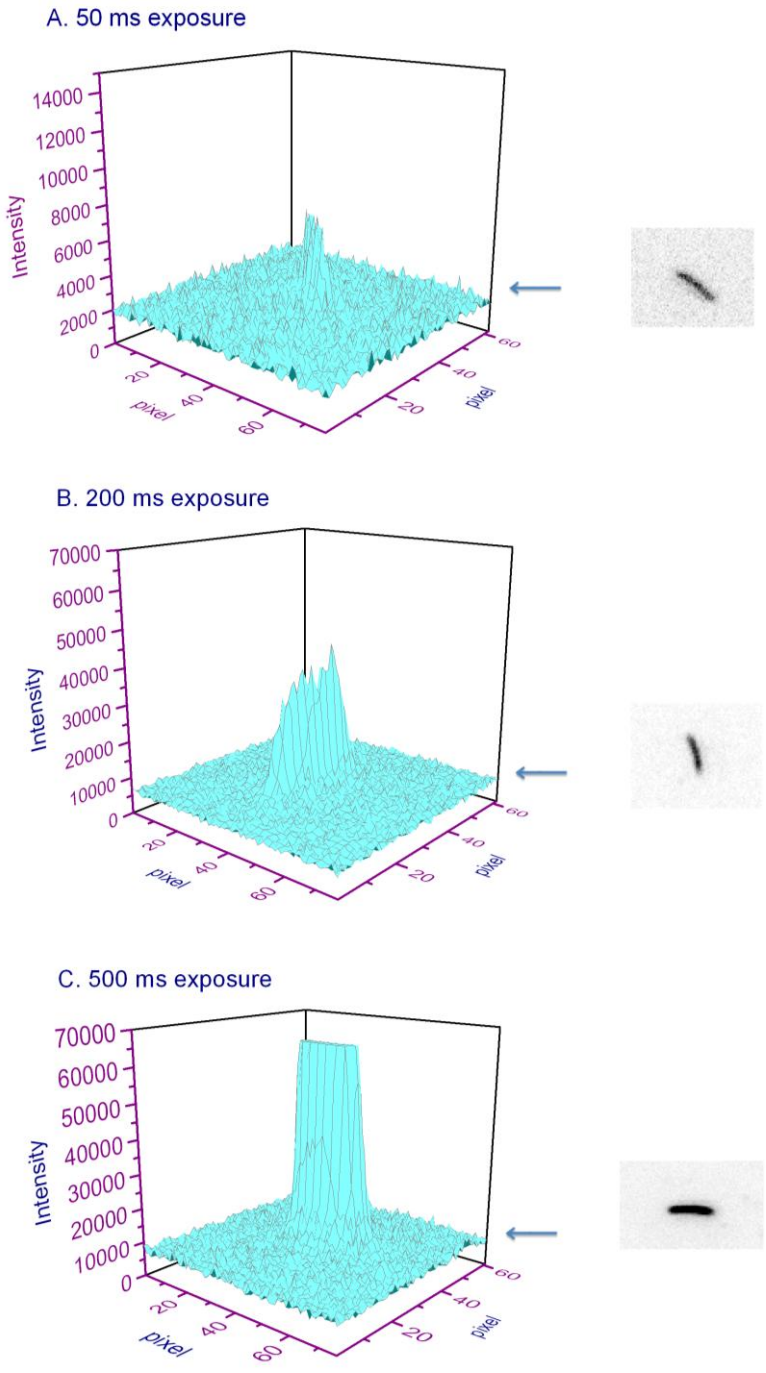

Figure S3. 3D plots showing the difference in signal to noise ratio for sampling rates 20 Hz (A), 5 Hz (B) and 2 Hz (C). The units of X and Y axes are pixels, the unit of Z-axis is intensity (arbitrary units). Threshold for background fluorescence elimination is indicated by the blue arrow. The corresponding inverted image is shown along each 3D plot.

Choice of acquisition rate: Ideally, for an actin filament moving uniformly along a straight line, the mean velocity does not depends on the rate of acquisition; however filament movement is complicated in a random way by curved paths, occasional hesitations etc. The use of a high sampling rate for a slow moving filament leads to poor estimate of the centroid due to the system noise. The use of a low sampling rate for a rapidly moving filament leads to an underestimate of the velocity, because the curved paths of filament are missed. The acquisition rate was chosen so that in consecutive frames there was always overlap between images of the moving filament and the centroid shift was at least one third the filament length.

Sampling rate	SD/mean	Minimum distance
20 Hz	<0.5	>2 μm
5 Hz	<0.3	>2 μm
2 Hz	<0.2	>2 μm

Table S2. Characteristic parameters for selection of the filaments.

Criteria for the selection of the filaments. To be considered representative of the sliding velocity *in situ*, the filament movement had to match a quality level established according to the following two criteria (Homsher et al., 1992): (*i*) a minimum distance of continuous movement (>2 μm) and (*ii*) a maximum value (cut-off) of the ratio SD/mean, that is 0.5 or 0.3 or 0.2 depending on the framing rate, 20 Hz or 5 Hz or 2 Hz respectively (Table S2, number of data points ≥8).

Figure S4 shows an example of V_F calculated frame-to-frame on a sequence of images, acquired at 20 Hz sampling rate, for a filament that stopped moving and then resumed the movement. During the first part of the trace (identified by the yellow line) the filament moved for ~8 μm with a noise defined by the SD/mean ratio of 0.21, that is quite below the threshold chosen as cut-off. During the middle part of the trace (identified by the red line) the filament stopped and then resumed sliding with a SD/mean ratio of 0.51, that is above the cut-off value and therefore it was excluded from the analysis. During the last part of the trace (identified by the green line) the filament slid for ~5.5 μm with a SD/mean ratio of 0.09. The continuous sliding over many actin filament lengths, occurring during the first and last part of the trace, is the result of the asynchronous action of the myosin molecules spread over the surface of the flow cell and reproduces the properties of the myosin molecules in situ. At least twenty filaments with such smooth sliding were selected from each slide.

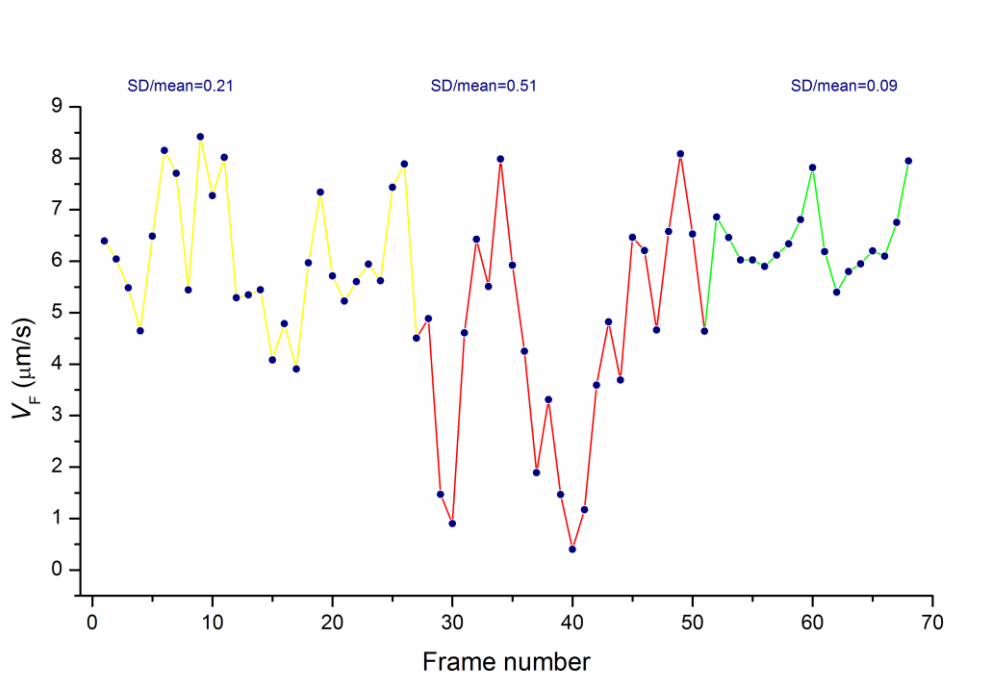

Figure S4. Sliding filament velocity (V_F), determined frame-to-frame, plotted against the frame number for an actin filament acquired at 20 Hz sampling rate. Different periods of the filament movement (marked by the colour of the line joining the points) were analysed separately. SD/mean ratio is 0.21 for the yellow line, 0.51 for the red line and 0.09 for the green line.

4. V_F versus storage time.

One main limit for the use of frog myosin in IVMA was its rapid deterioration. We tested the liability of our preparation by measuring V_F from the same preparation during the week following the extraction. The results are shown in Figure S5. The average V_F from the data collected in the first day, 5.38 ± 0.13 (mean ± SE, 4 slides), is not significantly different from that obtained from data collected the seventh day, 5.00 ± 0.09 (3 slides).

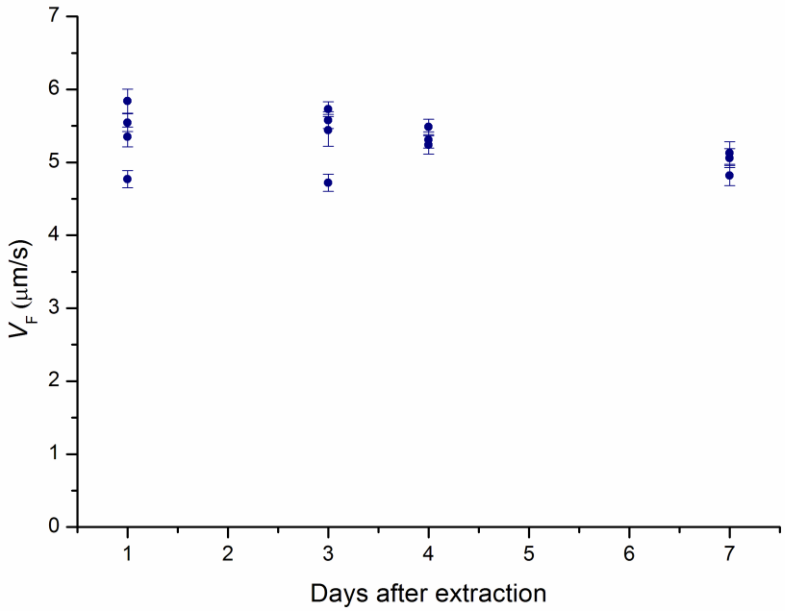

Figure S5. V_F determined in control experimental conditions is plotted against the days after the myosin extraction. Each point (mean ± SE) is the result of the analysis made on one slide with at least 20 filaments measured.

5. Effect of filament length.

Under conditions of saturating density of myosin molecules, V_F is expected to be independent of the filament length (Toyoshima et al., 1990; Uyeda et al., 1990). We tested this property in our IVMA under control conditions, plotting V_F for individual filaments (data from Figure 2B) versus filament length (Figure S6). We found no correlation between V_F and filament length (r = 0.22, linear regression coefficient = 0.00046 ± 0.00036).

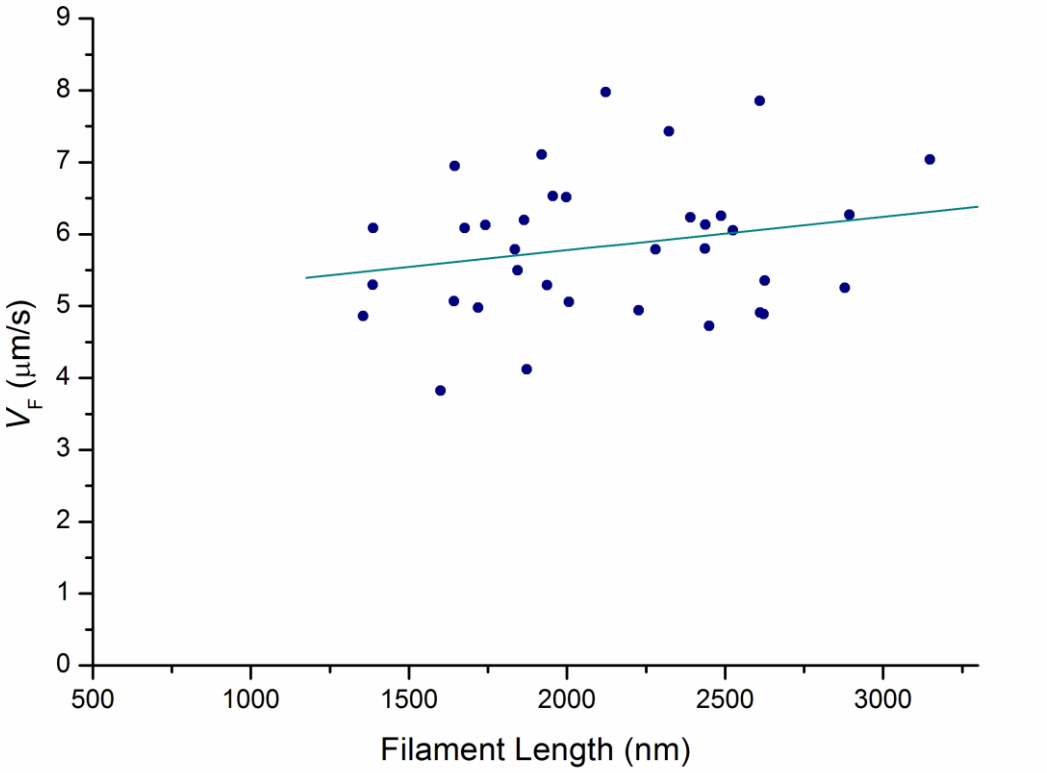

Figure S6. Sliding velocity of individual filaments versus the length of the filament. The continuous line is the linear regression equation. Data from Figure S2B.